

The effect of hydrostatic pressure on the electronic properties of TlBr and TlCl radiation detectors

N. Amrane and M. Benkraouda*

Department of Physics

United Arab Emirates University, Al-Ain, P.O. Box: 17551, U.A.E.

Abstract

We present first principles calculations of the electronic properties of TlBr and TlCl binary semiconductor compounds. The dependences on hydrostatic pressure of these properties (band structure, density of states, electronic charge density) are successfully calculated using self-consistent scalar relativistic full potential linear augmented plane wave method (FP-LAPW) within the generalized gradient approximation (GGA). The GGA corrections yield only minor improvement, whereas Engel-Vosko approximation gives a significant improvement to the band gap. The results are compared with previous calculations and with experimental measurements, we found good agreement with our calculations.

Keywords: band structure, density of states, electronic charge density, radiation detectors.

* Corresponding author.

Email: namrane@uaeu.ac.ae

Tel: (971) 505135896

1-INTRODUCTION

Thallium halides (TlCl and TlBr) are technologically very important materials having many applications as radiation detectors and as new optical fibre crystals. Thallium chloride and thallium bromide both, crystallize in the cubic CsCl structure. This structure, with a coordination number of eight, represents the most stable dense configuration for ionic crystals [1–3].

In the past two decades there has been much interest in the pressure dependence of the optical properties semiconductors [4-9]. While the fundamental understanding of this problem is in itself of great importance, with the recent development of strained superlattices it has become more relevant.

High-pressure studies are a very efficient tool in understanding the electronic and optical properties of semiconductors [10], but they have been scarcely used in the investigation of TlBr and TlCl, compared to other II–VI semiconductors. The study of materials at high pressures has become very important has a great activity because of the developments of the diamond-anvil technique and the extension of the range for optical and X-ray measurements under static pressures [11,12].

The main motivation of this work is to study the change in the optical properties under pressure of two technologically important semiconductors TlBr and TlCl. A modification of the crystal lattice which does not change its symmetry properties can be obtained by applying hydrostatic pressure to the crystal. Pressure changes produces shifts of the electronic states and, hence a change in the optical properties of the crystal. Therefore pressure provides a convenient technique for modifying optical constants by a controlled amount.

Most of the heavy-metal halides crystallize into anisotropic or layered structures. The simple lattice structure would reduce the complexity of electronic structure usually encountered in anisotropic materials and allows us a simple analysis of the optical spectra. Optical properties of TlCl and TlBr have been studied by many workers in the absorption edge [13] and in the VUV region [14]. A remarkable property of thallium halide crystals is their high dielectric permittivity. The static values are 30 and 32 for the cubic TlBr and TlCl [15-16].

In this study, we have investigated the optical properties by means of first-principles density-functional total-energy calculation using the all-electron full potential linear augmented plane-wave method (FPLAPW) [17].

2- CALCULATIONS

The calculation of the effect of pressure on the optical properties is a long standing problem in semiconductor physics. Although detailed calculations of the pressure dependence of optical properties with varying degree of sophistication like empirical pseudopotential [18], self-consistent first principle pseudopotential [19,20] and quasiparticle [21,22] have successfully estimated some coefficients, the results are not entirely satisfactory.

A modification of the crystal lattice which does not change its symmetry properties can be obtained by applying hydrostatic pressure to the crystal. Pressure changes the lattice parameters and, hence produces shifts of the electronic states in the crystal.

Scalar relativistic calculations have been performed using the wien2k code [23,24]. For the exchange correlation potential, we have used the local density approximation (LDA) with a parameterization of Ceperly-Adler data [25]. The new Full Potential Augmented Plane Wave method of the density functional theory is applied [26,27]. Several improvements to solve the energy dependence of the basis set were tried but the first really successful one was the linearization scheme introduced by Andersen [28] leading to the linearized augmented plane wave (LAPW) method. In LAPW, the energy dependence of each radial wave function inside the atomic sphere is linearized by taking a linear combination of a solution u at a fixed linearization energy and its energy derivative \dot{u} computed at the same energy.

$$\Phi_K(\mathbf{r}) = \begin{cases} \sum_L \left[a_L^{\alpha K} u_l^\alpha(\mathbf{r}') + b_L^{\alpha K} \dot{u}_l^\alpha(\mathbf{r}') \right] Y_L(\hat{\mathbf{r}}') & \mathbf{r}' \in R_\alpha \\ \Omega^{-1/2} \exp(i(\mathbf{k} + \mathbf{K}) \cdot \mathbf{r}) & \mathbf{r} \in I \end{cases} \quad (1)$$

Where $\mathbf{r}' = \mathbf{r} - \mathbf{r}_\alpha$ is the position inside sphere α with polar coordinates r' and \mathbf{r} , \mathbf{k} is a wave vector in the irreducible Brillouin zone, \mathbf{K} is a reciprocal lattice vector and u_l^α is the numerical solution to the radial Schrodinger equation at the energy ε . The coefficients $a_L^{\alpha K}$ are chosen such that the atomic functions for all L components match (in value) the PW with \mathbf{K} at the Muffin tin sphere boundary. The KS orbitals are expressed as a linear combinations of APWs $\Phi_K(\mathbf{r})$. In 1991 Singh [29] introduced the concept of local orbitals (LOs) which allow an efficient treatment of the semi-core states. An LO is constructed by the LAPW radial functions u and \dot{u} at one energy ε_1 in the valence band region and a third radial function at ε_2 .

$$\Phi_{LO}(\mathbf{r}) = \begin{cases} \left[a_L^{\alpha, LO} u_{ll}^\alpha(\mathbf{r}') + b_L^{\alpha, LO} \dot{u}_{ll}^\varepsilon(\mathbf{r}') + c_L^{\alpha, LO} u_{2l}^\alpha(\mathbf{r}') \right] Y_L(\hat{\mathbf{r}}') & \mathbf{r}' \in R_\alpha \\ 0 & \mathbf{r} \in I \end{cases} \quad (2)$$

Recently, an alternative approach was proposed by Sjöstedt et al [30], namely the APLW+ lo (local orbital) method. Here the augmentation is similar to the original APW scheme but each radial wavefunction is computed at a fixed linearization energy to avoid the non-linear eigenvalue problem. The missing variational freedom of the radial wavefunctions can be recovered by adding another type of local orbitals (termed in lower case to distinguish them from LO) containing u and \dot{u} term:

$$\Phi_{l_0}(\mathbf{r}) = \begin{cases} \left[a_L^{\alpha, l_0} u_l^{\alpha}(\mathbf{r}') + b_L^{\alpha, l_0} \dot{u}_l^{\alpha}(\mathbf{r}') \right] Y_L(\mathbf{r}') & r' < R_{\alpha} \\ 0 & r \in I \end{cases} \quad (3)$$

It was demonstrated that this new scheme converges faster than LAPW. The APW +lo scheme has been implemented in the wien2k code version [31].

However, in the calculations reported here, we chose the muffin tin radii for Tl, Br and Cl to be 2.5 a.u.. The expansion of the spherical region is developed up to $l_{\max}=10$ for both compounds, while in the interstitial region we have used 372 plane waves for TlBr and 331 for

TlCl. Furthermore, we have used the energy cut-off of $R_{MT} \cdot K_{\mu\alpha\xi}=8$ and the maximal reciprocal vector equal to 10 for both compounds.

3. RESULTS

The structural optimization of the cubic phase was performed by calculating the total energy as function of the volume. The minimization of the total energy versus volume requires that each of the self-consistent calculations is converged, so the iteration process was repeated until the calculated total energy of the crystal converged to less than 1 mRyd. A total of seven iterations were necessary to achieve self-consistency for TlBr and nine iterations in the case of TlCl. The equilibrium lattice constants and bulk modulus are calculated by fitting the total energy versus volume according to Murnaghan's equation of state [33]. The variation of total energy as a function of volume is shown in figures 1a and 1b for TlBr and TlCl respectively.

Our results are shown along with other theoretical values in Tables 1 and 2. It is found that for the generalized gradient approximation (GGA92) and (GGA96), the energy gap is underestimated relative to the experimental value due to the well known artifact of the local density approximation calculations, while the Engel-Vosko scheme gives quite a nice band gap compared to the experimental one.

3.1 Electronic band structures

The electronic band structures of cubic TlBr and TlCl along symmetry lines are shown in figures 2a, 2b at normal pressure and 3a, 3b under hydrostatic pressure. The calculated band energy gap at high symmetry points is given in table 2; the band gap is found to be direct and equal to 1.87 eV and 2.08 eV for TlBr and TlCl respectively, which is in close agreement with other theoretical calculations as shown in table 2.

It is clear from these figures that the energy levels are shifted upon applied pressure for both Tl Br and TlCl; under pressure, the energy levels for the valence bands decrease while the ones of the conduction bands increase, the main band gaps are also increased under pressure, hence The valence bandwidth increases with the increase of pressure, while the conduction bandwidth decreases with the increase of pressure.

The band structure is qualitatively similar to that of ambient pressure. However, the conduction minimum at C shifts upwards, while the X-point conduction-band minimum moves down

relative to the valence-band maximum. The energy of the lowest conduction band at the L point is almost independent of pressure.

We applied a pressure up to 8.69 GPa for TlBr and 10.33 GPa for TlCl, because this structure transforms to another phase when pressure exceeds those values. The variation is not constant and depends on the k-point and energy. Both materials under study remain a direct band-gap at 8.69 GPa for TlBr and 10.33 GPa for TlCl.

It is interesting to compare our calculated gaps with experimental data (see table 2). Since quasi-particle excitations are not taken into account in density functional theory (DFT), the energy gap calculated from DFT, often called the Kohn-Sham gap, tends to be smaller than the experimental one. In some cases, even the wrong ground state is predicted, as, e.g., in Ge, where the energy gap is around 0.7 eV, whereas the LDA Kohn-Sham gap is slightly negative at ambient pressure [26]. The GGA corrections yield only minor improvement. Quasiparticle calculations essentially overcome the underestimate of the band gap as obtained using the LDA. The GW [27] calculations for GaN for instance yield band structures in much better agreement with experiment; they are, however, time consuming and do not, as yet, produce selfconsistent total-energy values. However, in our case, the use of the Engel-Vosko improves significantly the band gap which becomes closer to the experimental one.

Figure 2a indicates that TlBr with cubic structure has a direct band gap between the top of the valence band and the bottom of the conduction band at the X. The lowest band is the Tl 6s-band. At X there is significant mixing between the nominal Tl s and the X_6^+ which is the valence band edge. A maximum pressure of 8.69 GPa was used.

In the case of TlCl (figure 3a), the overall results are similar to TlBr; table 2 summarizes the key information for TlCl, discrepancies between calculated and experimental band gap, which can be attributed as stated earlier to the exchange GGA potentials which do not take into account the excitations, whereas the Engel-vosko correction significantly improves the gap which is 2.72 eV and 2.96 eV for TlBr and TlCl respectively different from the experimental ones. Note that in the case of TlCl, the Cl s and p bands make the convergence of the calculation a bit longer. The calculated band gaps at $p = 8.69$ GPa and $p = 10.33$ GPa for TlBr and TlCl are given in table 3.

Table 1. Band energies (eV) and static equilibrium constant a (Å) for TlBr and TlCl

TlBr	Present work			Other calculations	Experiment
	GGA96	GGA92	Engel-Vosko		
Energy gap (eV)	1.87 eV at P=0 GPa 0.76 eV at P=8.69 GPa	1.74	2.72	2.38 (OPW) ^c	2.68 ^d
Lattice constant (Å)	4.0			3.96 ^c	3.98 ^a
TlCl	Present work			Other calculations	Experiment
	GGA96	GGA92	Engel-Vosko		
Energy gap (eV)	2.08 eV at P= 0 GPa 0.87 eV at P=10.33 GPa	1.94	2.96	2.04 (OPW) ^c	3.22 ^d
Lattice constant (Å)	3.84	---	---	3.84 ^c	3.83 ^b

^areference [28]^breference [29]^creference [30]^dReference [31]

3.2 Total charge density

To visualize the nature of the bond character and to explain the charge transfer and the bonding properties of cubic TlBr and TlCl, we calculate the total charge density.

The electronic charge density is obtained for each band n by summing over the k -states in the band.

$$\rho_n(r) = \sum_k |\Psi_{nk}(r)|^2 \quad (6)$$

and the total charge density is obtained by summing over the occupied band.

$$\rho(r) = \sum_n \rho_n(r) \quad (7)$$

The total valence charge densities for the two binary compounds, TlBr and TlCl, are displayed along the Tl-Br-Cl bonds in figures 3a and 3b.

Figures 4a and 4b show the charge density distribution in the (110) plane for TlBr and TlCl respectively at normal pressure and at 8.69 GPa for TlBr and 10.33 GPa for TlCl. The calculated electron charge distributions indicate that there is a strong ionic character for both

compounds as can be seen along the Tl-Br-Cl bonds. The charge densities around the atoms have asymmetric forms which are similar to those given in previous reports using the ab initio pseudo-potential method [32]. The charge transfer gives rise to the ionic character in TlBr and TlCl semiconductor compounds. The driving force behind the displacement of the bonding charge is the greater ability of Tl to attract electrons towards it due to the difference in the electronegativity of Tl and Br. However as pressure is applied we note a charge transfer toward the interstitial region, and also a decrease in the charge density, more noticeable in the case of TlBr, this is attributed to the difference in the core size of these compounds. The charge distribution which was concentrated at the atomic sites at normal pressure becomes more delocalized throughout the unit cell. This difference has important physical consequences, the substitution of the interstitial sites of TlBr and TlCl with host atoms can affect the band structure topology and gives rise to a semiconductor with new physical properties.

The total DOS curves displayed on figures 5a and 5b give an idea about the dominant orbital character of the groups of bands in the indicated regions of energy for TlBr and TlCl, respectively.

The cubic binary compounds TlBr and TlCl have valence band densities of states qualitatively similar to the band structures. The energy zero is the top of the valence band, E_v , or valence-band maximum (VBM). Structures of the density of states are labeled with the same notation as the band structure and the corresponding points in the Brillouin zone follow from inspection of the band structure. The minimum of the density of states occurs at Γ at -5.3 eV for TlBr and -5.2 eV for TlCl. The lower states from -5.3 to -2.7 eV and from -5.2 to -2.71 eV for TlBr and TlCl, respectively have primarily s character and are localized on the anion. The second state of the second valence band is cation s, it changes rapidly to anion p-like at the top of the valence band in the case of TlCl. However, as pressure is applied, the intensity of the peaks in the DOS figure decreases and also both valence and conduction band peaks are shifted as stated above in the band structure analysis.

Conclusion

The effect of hydrostatic pressure on the electronic properties of cubic TlBr and TlCl have been investigated using the wien2k package, full-potential linearized augmented plane wave (FP-LAPW) approach within the density functional theory (DFT) in the local spin density approximation (LSDA) including the generalized gradient approximation (GGA) was used. The use of GGA for the exchange-correlation potential permitted us to obtain good structural parameters but an underestimated fundamental band gap, whereas the Engel-vosko correction significantly improves the gap. The charge densities have been presented and provide additional evidence of the similarity of the bonds in TlBr and TlCl. As a result of the ionic character of these two binary semiconductor compounds which share many similar properties. We noticed that at much lower pressures, the character of the fundamental gap is affected by changes in band dispersion of the topmost part of the valence band in both TlBr and TlCl.

However, the charge distribution which was concentrated at the atomic sites at normal pressure becomes more delocalized throughout the unit cell as pressure is applied, this has important physical consequences, substitution of the interstitial sites with host atoms will give rise to a semiconductor with different physical properties.

Acknowledgment:

P. Blaha, K. Schwarz, G. Madsen, D. Kvasnicka and J. Luitz, *WIEN2k*, An Augmented Plane Wave + Local Orbitals Program for Calculating Crystal Properties (Karlheinz Schwarz, Techn. Universität Wien, Austria), 2001. ISBN 3-9501031-1-2

Figure captions

Figure 1a: Energy (eV) versus Volume (\AA^3) for TlBr

Figure 1b: Energy (eV) versus Volume (\AA^3) for TlCl

Figure 2a: Energy (eV) versus Wave vector for TlBr at normal pressure (GGA-08)

Figure 2b: Energy (eV) versus Wave vector for TlCl at normal pressure (GGA-08)

Figure 3a: Energy (eV) versus Wave vector for TlBr at pressure $p=8.69$ GPa, (GGA-08)

Figure 3b: Energy (eV) versus Wave vector for TlCl at pressure $p=10.33$ GPa, (GGA-08)

Figure 4a: Electron density (arb. Units) versus Position (a.u.) for TlBr at normal pressure and at $p=8.69$ GPa (GGA-08)

Figure 4b: Electron density (arb. Units) versus Position (a.u.) for TlCl at normal pressure and at $p=10.33$ GPa (GGA-08)

Figure 5a: Density of states for TlBr at normal pressure and at $p=8.69$ GPa (GGA-08)

Figure 5b: Density of states for TlCl at normal pressure and at $p=8.69$ GPa (GGA-08)

REFERENCES

- [1] C.W.F.T. Pistorius, J.B. Clark, Phys. Rev. 173 (3) (1968) 692–699.
- [2] R.M. Brade, B. Yates, J. Phys. C: Solid State Phys. 4 (1971) 417–427.
- [3] W.N. Lawless, Phys. Rev. B 30 (10) (1984) 6057–6066.
- [4] J.A. Sansa, A. Seguraa, F.J. Manjonb, B. Marib, A. Munoz, M.J. Herrera-Cabrera Microelectronics Journal 36 (2005) 928–932
- [5] Alouani M., Brey L., Christensen N.E. Phys. Rev. B, 37 1167-79, 1988.
- [6] Chen, Wei ; Zhang, Jin Z. ; Joly, Alan G.
Journal of Nanoscience and Nanotechnology; Journal Volume: 4; Journal Issue: 8
2004.142.
- [7] A. Seguraa, J. A. Sans, A. Munoz and M. J. Herrera-Cabrera
APPLIED PHYSICS LETTERS VOLUME 83, NUMBER 2 14 JULY 2003.
- [8] L. Kalarassea, A. Melloukia, B. Bennecer, and F. Kalarasse
Journal of Physics and Chemistry of Solids Volume 68, Issue 12, December 2007, Pages 2286-2292
- [9] F. Benmakhlouf International Journal of Modern Physics B Vol. 20, No. 28 (2006) 4807–4820.
- [10] R. A. Secco et al. Solid State Communications Volume 107, Issue 10, 29 July 1998, Pages 553-556.
- [11] W. B. Holzapfel, Rep. Prog. Phys. 59, 29 (1996) .

- [12] J. V. Badding, *Annu. Rev. Mater. Sci.* 28, 631 (1998) and references therein.
- [13] M. Ueta, H. Kanzaki, K. Kobayashi, Y. Toyozawa and E. Hanamura, *Excitonic Processes in Solids*, ed. M. Cardona, P. Fulde, K. von Klitzing and H.-J. Queisser (Springer, Berlin, 1986) Springer Ser. Solid-State Sci. 60, p.370.
- [14] K. Soda, A. Mikuni, H. Kanzaki and T. Ishii, *Core-Level Spectroscopy in Condensed Systems*, ed. J. Kanamori and A. Kotani (Springer, Berlin, 1988) Springer Ser. Solid-State Sci. 81, p.222.
- [15] V. F. Agekyan and Yu. A. Stepanov, *Physics of the Solid State*, Vol. 43, No. 4, 2001, pp. 763–765.
- [16] Landolt-Börnstein, *Non-Tetrahedrally Bonded Elements and Binary Compounds I Vol.III* (1998).
- [17] B. Daoudi, M. Sehil, A. Boukraa, H. Abid *Int. J. Nanoelectronics and Materials* 1 (2008) 65-79.
- [18] P. Friedel, M. S. Hybertsen, and M. Schlüter *Phys. Rev. B* 39, 7974–7977 (1989).
- [19] Fan Wei-jun^{1,2}, Gu Zong-quan², Xia Jian-bai^{1,2} and Li Guo-hua² *Chinese Phys. Let.* Vol. No 6 (1992) 305.
- [20] Fan Wei-jun et al (1992) *Acta Phys. Sin.* 1 45.
- [21] F. Fuchs and F. Bechstedt, *Phys. Rev. B* 77, 155107 (2008)
- [22] Asier Eiguren, Claudia Ambrosch-Draxl, and Pedro M. Echenique *Phys. Rev. B* 79, 245103 (2009).
- [23] K.Schwarz, P.Blaha, G.K.H.Madsen, *Comput.Phys.Commun.* 147 (2002) 71
- [24] K.Schwarz, P.Blaha, *Comput.Mater.Sci.* 28 (2003) 259
- [25] D.M.Ceperley, B.I.Alder, *Phys.Rev.Lett.*45 (1990) 566
- [26] E.Wimmer, H.Krakauer, M.Weinert, A.J.Freeman, *Phys.Rev.B*24 (1981) 864
- [27] P.Blaha, K.Schwarz, P.Sorantin, S.B.Trikey, *Comput.Phys.Commun.*59 (1990) 399
- [28] O.K.Andersen, *Phys.Rev.B*12 (1975) 3060-3083.
- [29] D.Singh, *Phys.Rev.B* 43 (1991) 6388-6392.
- [30] E.Sjöstedt, L.Nordström, D.J.Singh, *Solid State Comm.*114 (2000) 15-20
- [31] P.Blaha, K.Schwarz, G.K.H.Madsen, D.Kvanicka, J.Luitz, WIEN2k, An Augmented Plane Wave Plus Local Orbitals Program For Calculating Crystal properties, Vienna University of Technology, Austria 2001.
- [32] H.J.Monkhorst, J.D.Pack, *Phys.Rev.B*13 (1976) 5188.
- [33] Murnaghan F D 1944 *Proc. Natl Acad. Sci. USA* 30 5390.
- [34] Vassilios Yannopapas and Alexander Moroz, *J. Phys.: Condens. Matter* 17 (2005) 3717–3734.
- [35] M. Ueta, H. Kanzaki, K. Kobayashi, Y. Toyozawa and E. Hanamura, *Excitonic Processes in Solids*, ed. M. Cardona, P. Fulde, K. von Klitzing and H.-J. Queisser (Springer, Berlin, 1986) Springer Ser. Solid-State Sci. 60, p.370.
- [36] Sakuragi et al, *Adv. in Cerm*; vol. 2, pp. 84-93, (1981)

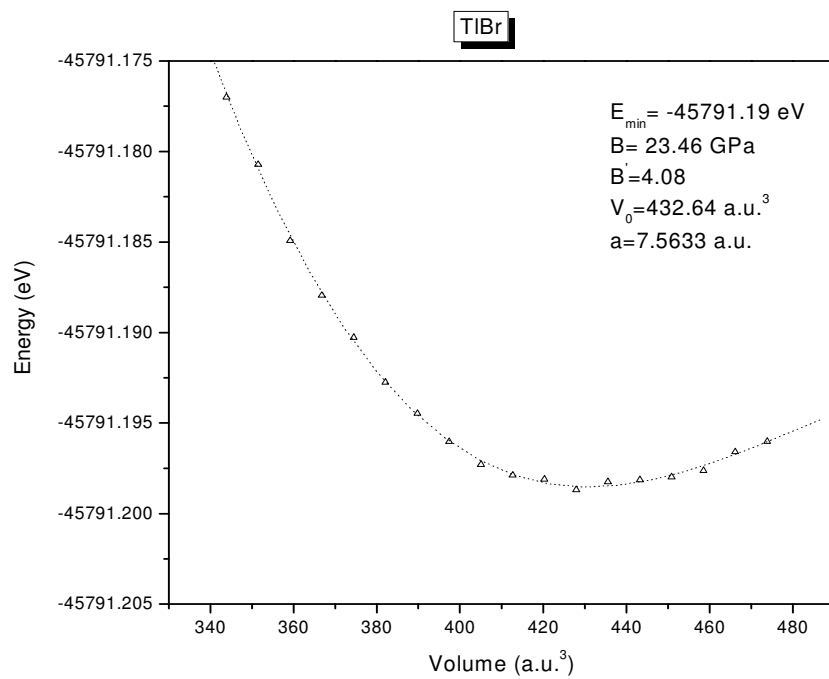


Figure 1a

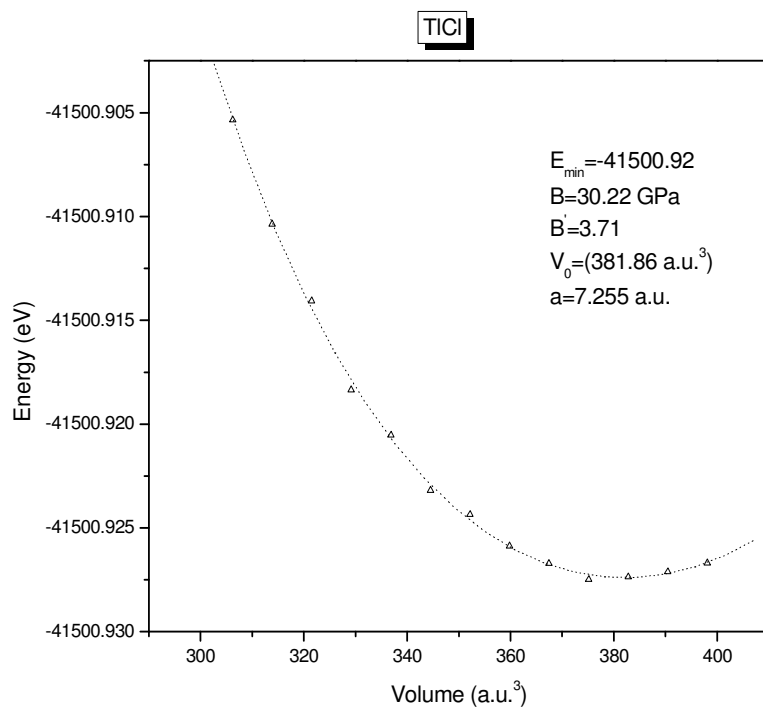


Figure 1b

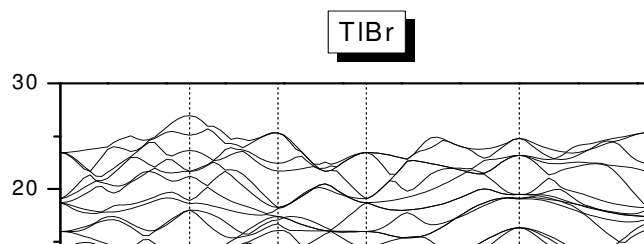


Figure 2a

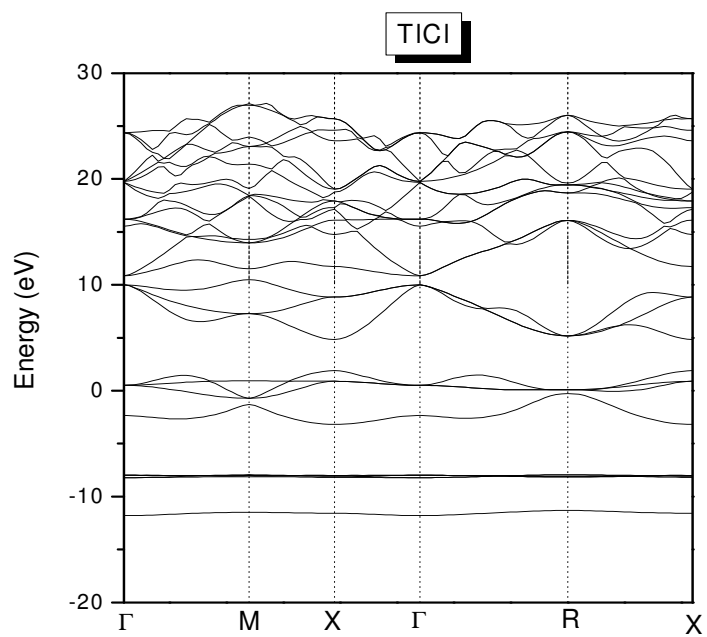


Figure 2b

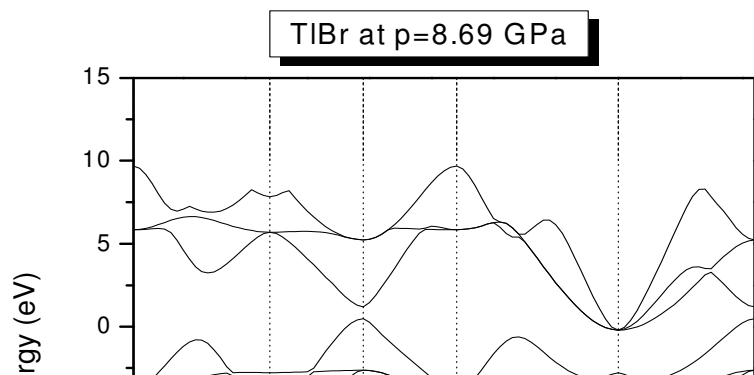


Figure 3a

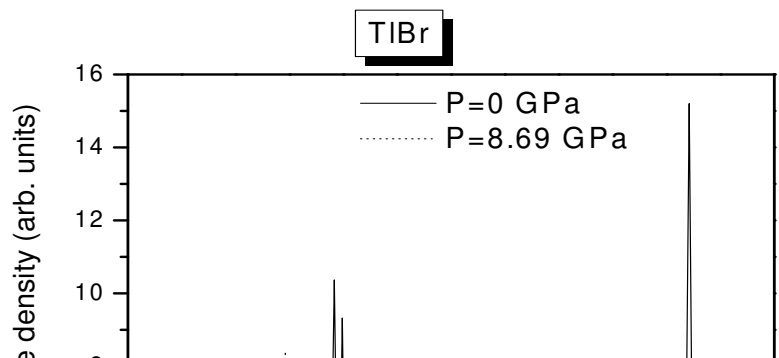
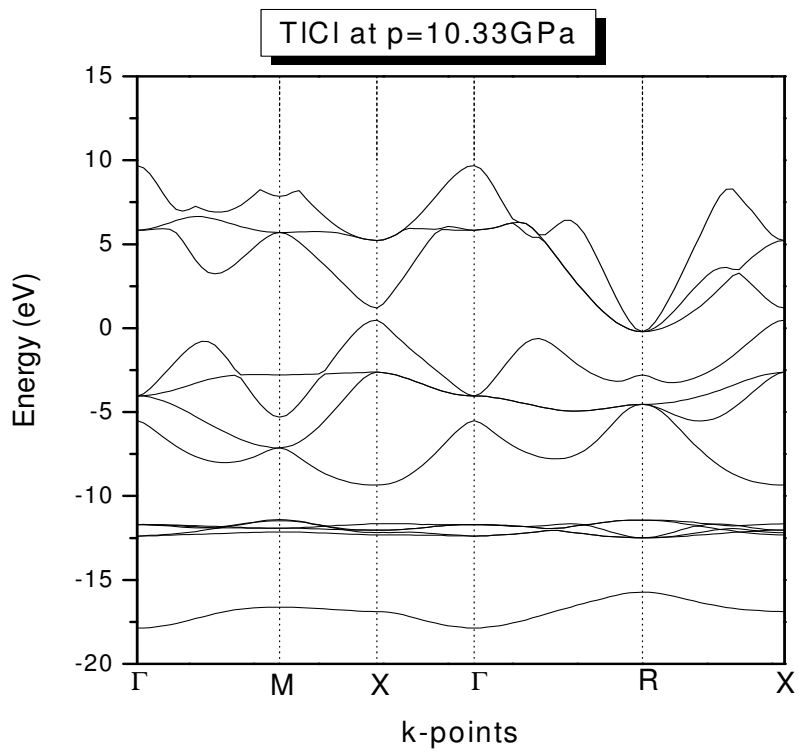


Figure 4a

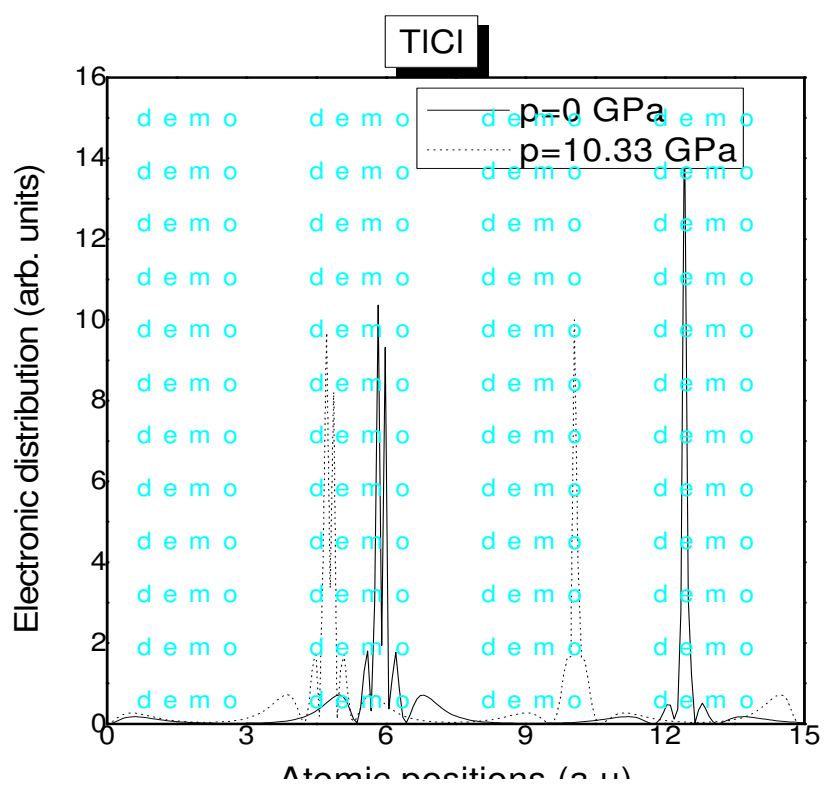


Figure 4b

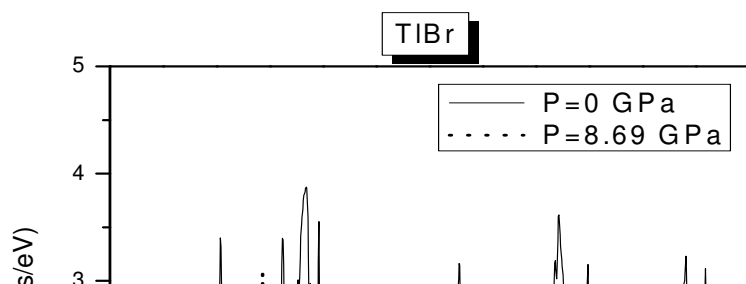


Figure 5a

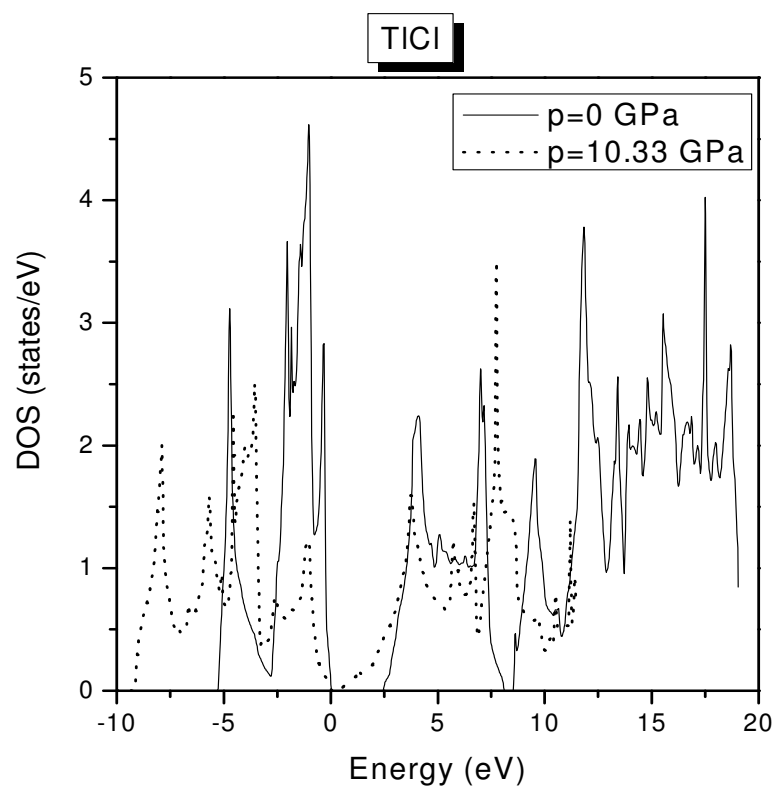


Figure 5b